SCALING OF HALFTONED IMAGES

Dan Chevion[*]*, Eugene Walach**
*Mike Stanich**, Larry Ernst**, Hong Li**, Joe Czyszczewski***

Keywords: Scanning, Printing, Publishing, Compression, Quality, Blue noise, Dot diffusion, Error diffusion, Halftoning, Inverse halftoning, Stochastic screening.

Abstract:

The goal of this paper is to describe technique for inverse screening halftoned images, created for an electrophotographic printer, and scaling the contone result. The objective is to achieve high quality results on another printer, for example an ink-jet printer. The approach we take is in the spatial domain. However, screen characteristics are determined in the frequency domain. Deducing screen attributes from the samples is possible and even quite robust. Test results yielded very good estimates. We found that for a 96 LPI screen at 51 degrees, where the spatial vectors for the screen are v1=4, 5 (horizontal, vertical) and v2=-4, 5 – the estimated parameters are in agreement with the data within 1.5%.

This means that we can identify the closest screen and use predefined data for our solution. For an unknown screen we can produce the data on the fly. Next step is to convolve the image with a flat filter (of only ones and zeroes) at the correct shape and size. This yields very nice results having excellent contone reconstruction which are better than a Gaussian low pass filter.

We'll show how this reconstruction procedure is connected to the actual halftone properties, thus fitting our intuition as well as human visual system (hvs) properties.

Next we scale the image to avoid moiré patterns at the contone level.

I. INTRODUCTION

Output of conventional printers tends to be binary (i.e. in the form of black dots). Hence, before the printing, gray level images must be pre-processed (half-toned). This process is called screening. There are many possible half-toning techniques. Naturally, every screening software module, works with one of the possible approaches optimized for the given printer.

Frequently, upon completion of the printing process, original gray-level images are discarded and only screened versions are retained. The problem arises when half-toning technique should be changed (e.g. due to the printer upgrade). In such cases, it is necessary to transform large volumes of screened images into a new printing (half-toning) standard.

One possible solution to this problem would be a reverse process, where screened images are translated back to their contone equivalents. Indeed, having a contone representation may be very useful for a number of reasons. For instance, halftone images are usually ill-suited to many common image processing procedures, such as compression, scaling, rotation, re-screening, or tone correction. As a result, descreening is usually the first step in the halftone image processing. Then, when image processing is completed, contone image can be half-toned again in a way optimal to the new printing device.

The technical question is: how do we extract contone images from their half-toned representations. Since half-toning process is irreversible, this is a non-trivial question. Moreover, since even small repetitive image distortions may cause very annoying display effects (so called Moiré patterns), it is essential to ensure very good reconstruction quality. In other words, it is essential to ensure that de-screened image would be a very good approximation of the gray-level original.

An intuitive approach to this problem is to apply low pass filtering in order to blend printing dots together. However, this approach tends to distort the edges of the objects creating an undesirable "out

---

* *IBM Research Division*
** *InfoPrint Solutions Company*

of focus effect”. Indeed, the basic aim of the inverse halftoning is to separate the halftoning noise from the original image. However, in good halftoning algorithms, the noise introduced by halftoning is blue, i.e., it is concentrated in the areas, where the original image is busy. Thus, simple low pass filtering that removes most of the halftoning noise, will also remove the edge information.

In addition to low-pass filtering, there are more sophisticated approaches to inverse halftoning. The method of *projection onto convex sets (POCS)* has been used by Analoui and Allebach [1] for halftone images produced by ordered dithering. POCS approach has been also used successfully by Hein and Zakhor [2] for error diffused halftones. A different method, called logical filtering, has been used by Fan [3] for ordered dither images. Wong [4] has used an iterative filtering method for inverse halftoning of error diffused images. Finally the method of over-complete wavelet expansions has been used in [5] to produce inverse halftones with good quality.

During the process of preparing this paper, we came across another promising (perhaps the fastest) method for inverse halftoning which uses space varying filtering based on gradients obtained from the image [6]. Another method [8] is a wavelet decomposition of the halftone images. This method facilitates a series of spatial and frequency selective processes that eliminate most of the halftone noise, while preserving most of the original image content. This approach lends itself to practical applications. Indeed, since it is independent of parameter estimation, it is applicable to all types of halftoned images, including those obtained by scanning printed halftones.

The purpose of this paper is to describe an investigation of a de-screening technique capable of exact elimination of the periodic patterns introduced by the clustered dot halftoning technique. Since halftoning itself is based on spatial integration of human vision it is only natural to descreen halftone images by averaging of the black and white pixels in a certain neighborhood around each pixel. However, if the shape and size of this averaging block is not identical to the shape and size of the basic halftone cell, the cell grid patterns will be visible, especially at uniform gray level areas. Hence, it is crucial to have precise estimates of the halftoning cell size and shape. In order to find these parameters, we've used the Fourier spectrum analysis of halftone images (similar approach has been also analyzed at [10]-[16])

It provides substantially better detail than the traditional low pass filtering approach, yet it is robust to noise and distortions. This technique has been developed for electronic images (so called orthographical halftone). However, in practice, it also works well for scanned halftone images.

The algorithm consists of the following three stages:

To begin with, screened images are analyzed in order to estimate the half-toning process parameters. The halftone image is viewed as the contone image sub-sampled at the lattice points. Fourier Transform (FT) converts such a lattice into its reciprocal form. FT of halftoned image can be viewed as a FT of the contone image convolved with the FT of the lattice. Accordingly, high peaks of the FT are located at the corresponding reciprocal lattice points. Detecting these peaks is equivalent to measuring the reciprocal spatial vectors. These vectors, in turn, can be converted back in order to compute the parameters of the original lattice. This technique was evaluated for halftones which are non orthogonal as well as orthogonal. In addition halftone which are AM/FM hybrid designs were included in the investigation.

In the second phase (reconstruction), these parameters are used to estimate the contone image samples. Various interpolation schemes have been explored including two-dimensional equivalents of “sample and hold” and linear interpolation algorithms.

The third step is to rescale images (if necessary). The scaling can be combined with the interpolation reducing computational load without compromising quality. Instead of computing the value of each pixel at the “source image” resolution, we compute only pixels needed for the “target image”. Up to 36% reduction in the computational complexity has been demonstrated.
We have tested this method on screened electronic images in resolutions of 240, 300 and 600 DPI. The original AFP data contained a mixture of text, halftone images, business graphics and line art with screen frequencies ranging from 42LPI at 240DPI, to 121LPI at 600 DPI, having orthogonal and non-

orthogonal orientations for the screen directions. The aim was to translate these images up to 360x360DPI and 720x720DPI 8 bit contone. In all cases excellent image quality has been achieved.

II. THE PROCESS

Ordered dither half toning techniques fall into two broad categories: clustered dot and dispersed dot [9]. In this work we have focused on the clustered-dot approach. It is widely used in the mass hard copy publications produced by offset printing, such as in newspapers, magazines and books. Clustered-dot techniques are characterized by the use of patterns of dots that are nucleated in groups at regular intervals along two directions. Figure 1 illustrates an example of this type of halftone. For convenience of the display we have enlarged pixel size so that dithering patterns can be visible. In reality, dots would be much smaller creating a good quality impression of the smooth gray-level image.

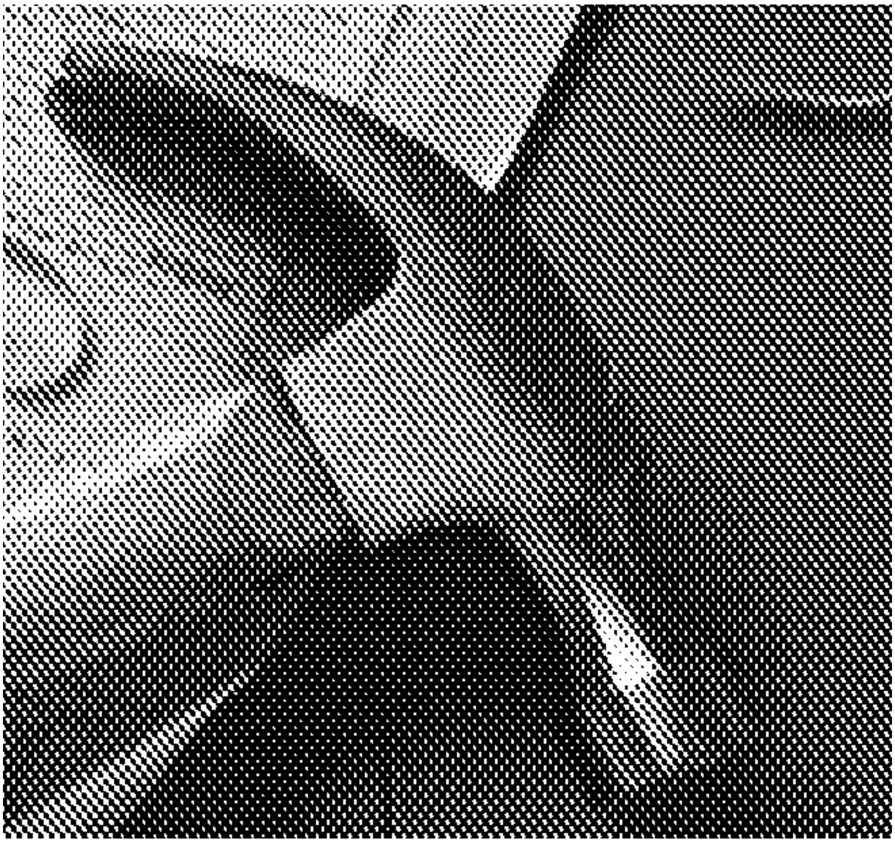

Figure 1: illustrates an example of clustered-dot type of halftone

Each halftone dot belongs to a screen cell. Screen cells may be collected together in a larger structure called a supercell. In general the shape of the cell is a parallelogram. In the illustration above the cell is a diamond. The shape of the cell is completely defined by two vectors (sides of this parallelogram). When these vectors are orthogonal to each other, rectangular cell is created. However, since human visual system is most sensitive to orientations at 0 and 90 degrees, prevailing halftoning techniques apply cells with 45 (or -45) degrees between the basic cell vectors. This optimal angle has been determined empirically from the earliest days of the halftoning.

In the sequel we'll focus on images created using no orthogonal cells. As explained in the introduction, we'll apply three-stage process

Phase I – Analysis.

The dots in a halftone image are ordered in a lattice called the screen grid. Each black halftone dot belongs to a single screen cell, and, for a linear lattice, the centers of the screen cells are located at the integer multiples of the basic spatial vectors.

We may think of a halftone image as a sub-sampled version of the contone image with samples taken at the lattice points (see also [11]). The lattice is a two dimensional grid, characterized by the two basic vectors $(a_1 \; and \; a_2)$, forming two of the four edges of a basic parallelogram cell. Thus a complete cell is formed by following the path a1, a2,-a1, and –a2. Figure 2 illustrates this pattern for halftone technique of 96 LPI/51 degrees, and non orthogonal screen.

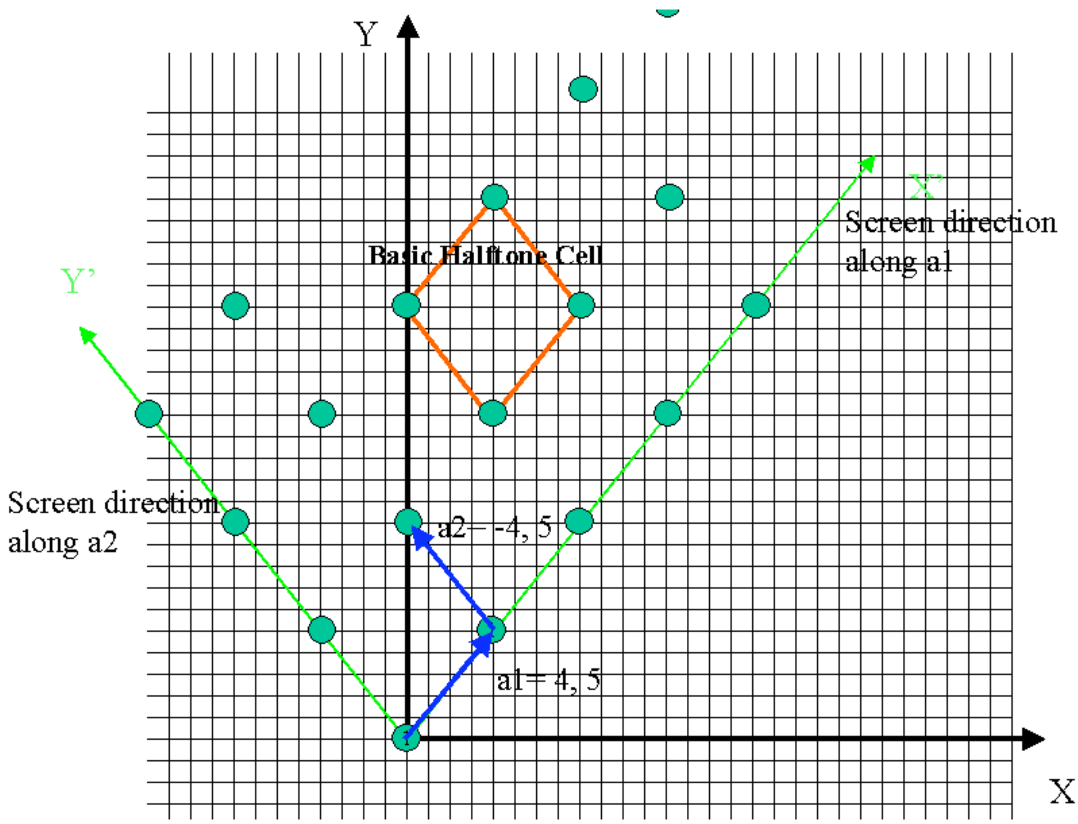

Figure 2: Spatial vector a1 and a2

Fourier transform converts such a lattice into its reciprocal form. Reciprocal lattice is characterized by two new base vectors in the frequency domain $(b_1 \; and \; b_2)$, These two sets of base vectors fulfill the "orthogonality requirement"

$a_i b_j = \delta_{ij}$, where δ_{ij} is the Kronecker Delta; (1)

In particular,

b_1 is perpendicular to a_2 and $|b_1| = N / |a_1| Sin(a_1 \wedge a_2)$ (2)

b_2 is perpendicular to a_1 and $|b_2| = N / |a_2| Sin(a_1 \wedge a_2)$ (3)

Where N is the length and width of the Fourier transform image.

Fourier transform of a halftoned image can be viewed as a Fourier transform of the contone image convolved by the Fourier transform of the lattice. Accordingly, high peaks in the Fourier transform are located at the corresponding reciprocal lattice points. Since those peeks are very high, relative to their neighborhood, it is fairly easy to detect them. Detecting those peaks is equivalent to measuring the reciprocal spatial vectors. Reciprocal base vectors can be, in turn, converted back in order to compute the parameters of the original lattice.

These considerations lead us to the following algorithm:

- Fourier transform of the halftone image is computed
  For this purpose, it is sufficient to take only a part of the image, provided it is large enough for the computation of the Fourier transform. In our experiments we have chosen to work with a 256 X 256 sub sample of the original image.
- Peaks on the transform are identified
  Since Fourier transform peaks are very pronounced, one can simply apply a thresholding technique with threshold being set to, say, 90% of the Fourier Transform Maximum. As a result we obtain several small blobs located at the vicinity of the origin of the Fourier transform image. Location of the peaks is computed as centers of these blobs.
- Transform grid is created
- Reciprocal of the transform grid is computed
  with every edge perpendicular to its counter part in the transform grid. Due to the transform duality, reciprocal of the transform grid constitutes a good approximation of the original grid.

This algorithm yields excellent estimates of the spatial vectors a1 and a2.

Phase II – binary to contone conversion

Once spatial vectors are known, original binary image can be reconstructed by convolving screened image with the cell mask.

In addition, it may be useful to perform low pass filtering by performing interpolation between neighboring pixels. One way to achieve this effect is by performing double interpolation with the same cell mask.

Note that this simple solution hinges on having precise cell size and shape estimates. Otherwise, grid would be noticeable, especially in the relatively flat areas ([12]).

Note that, usually, conversion process is performed at the original image resolution. Alternatively, one can increase both image and mask resolution in order to reduce some inherent image ruggedness. In our case we have experimented with doubling image resolution from 600 DPI to 1200 DPI (see Figures 4 and 5 below) .

Phase III – Scaling

The next step is to rescale the image in order to adapt it to the target printing device. In order to reduce computational complexity it is advantageous to combine the scaling with the convolution stage. Indeed, instead of computing convolution values for each pixel at the "source image", one can perform this computation only for the "target image" pixels. Hence, fast convolution is possible without compromising image quality.

III. EXPERIMENTAL RESULTS AND DISSCUSSION

We have implemented aforementioned system and run it on screened images at LPI=96, a1=(4,5) , a2=(-4,5) and angle of 51.3°. All the parameters where estimated correctly with accuracy within 1.5%

In Figures 3 and 4 reconstructed images are presented (with resolution 720 and 360 DPI respectively). In both cases virtually no grid effects are noticeable.

Next we have performed reconstruction with original image at 600 DPI and 1200 DPI (interpolated). Results appear at Figures 5 and 6. Figure 5 depicts results for 720 DPI target and Figure 6 depicts results for 360 DPI target. In both cases low resolution appears on the left and high resolution appears on the right. Under close inspection, it is clear that in both cases increased resolution yields somewhat better image quality. However, this improvement comes at the expense of increase computational load.

In order to perform comparison between different interpolation techniques, we have performed single and double convolution. Results are depicted in Figure 7 (for 720 DPI target) and Figure 8 (for 360 DPI target). Both interpolation techniques yield comparable image quality. As expected, double convolution provides better rendering of smooth areas at the expense of some degree of the edge distortion. In our judgment, double convolution quality does not justify increased computational load.

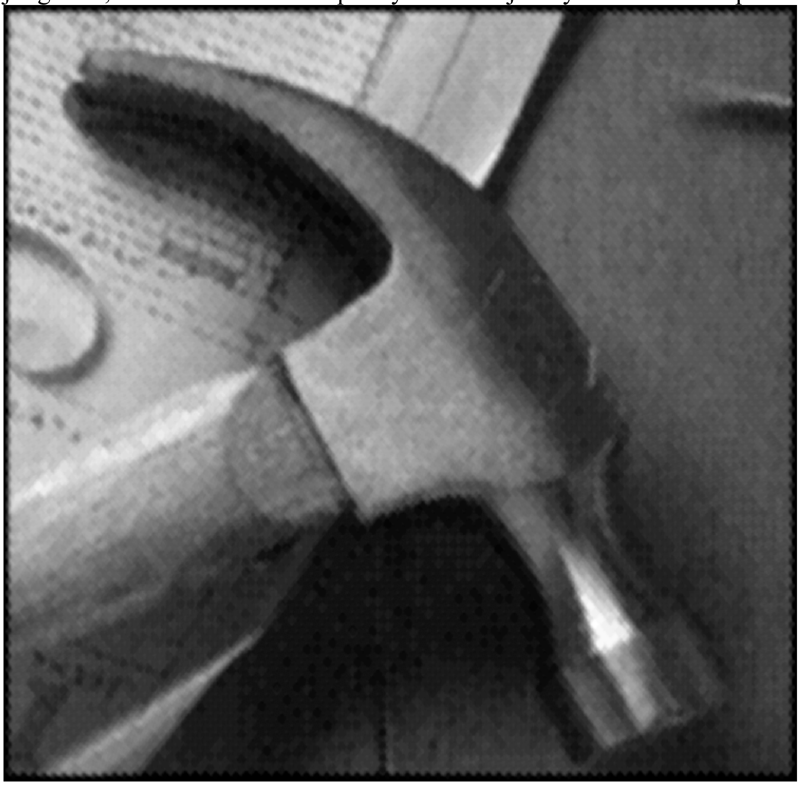

Figure 3: Reconstructed image at resolution of 720X720

Figure 4: Reconstructed image at resolution of 360X360

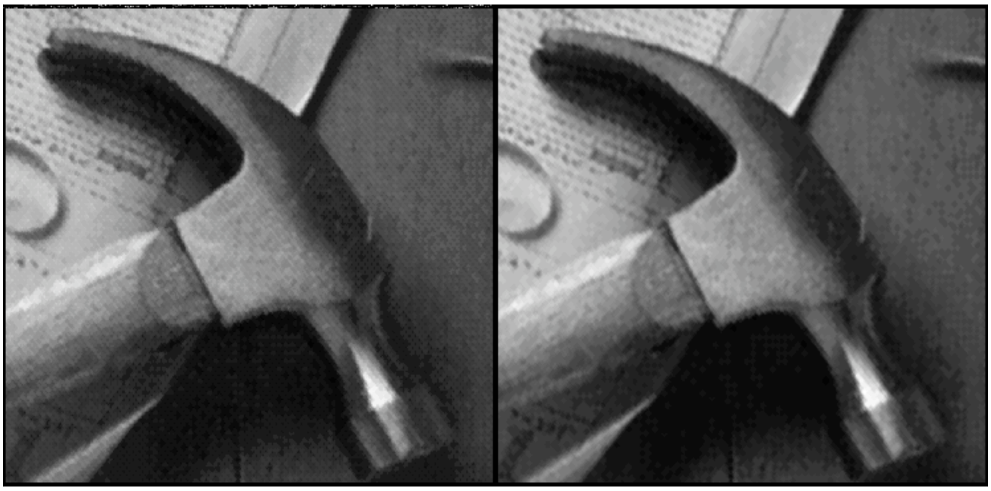

Figure 5: Reconstructed images for 360 DPI target with original images of 600 DPI (on the left) and 1200 DPI (on the right).

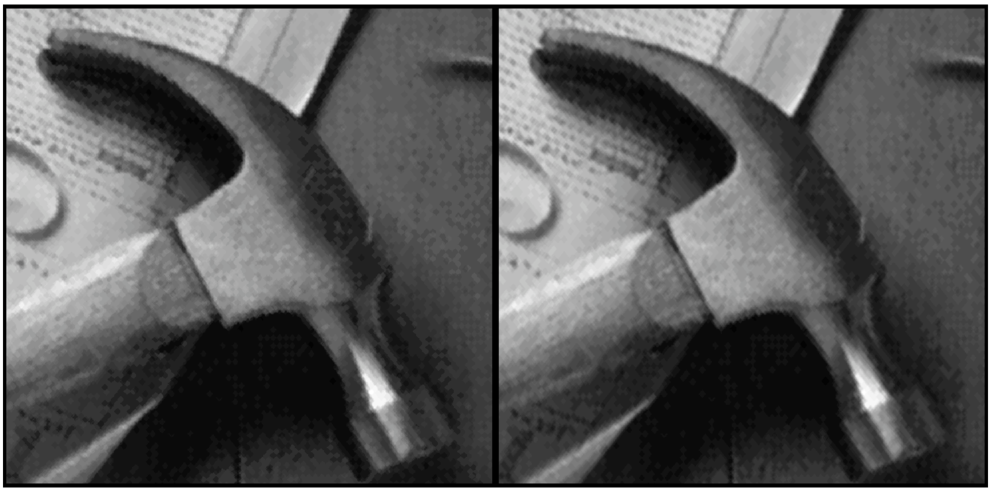

Figure 6: Reconstructed images for 720 DPI target with original images of 600 DPI (on the left) and 1200 DPI (on the right).

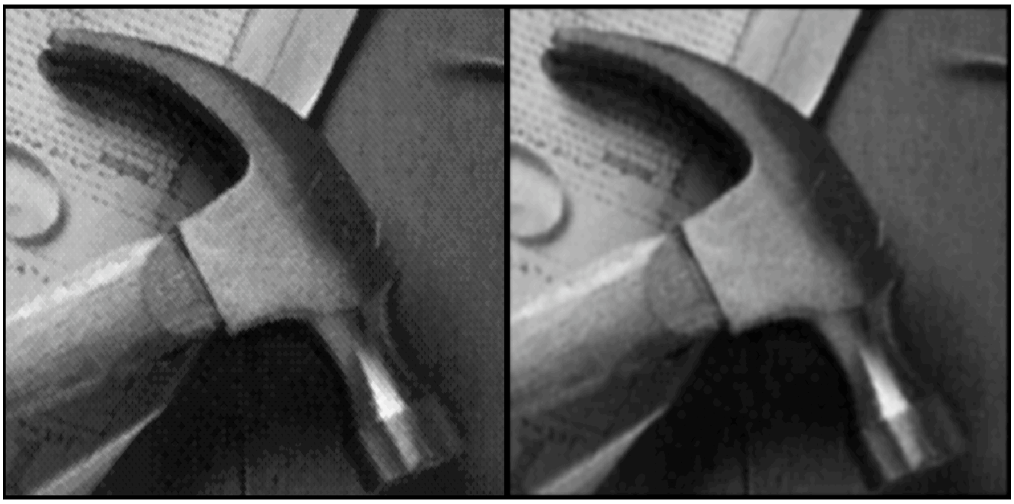

Figure 7: Reconstructed image for 720 DPI target. Single convolution (on the left) and double convolution (on the right).

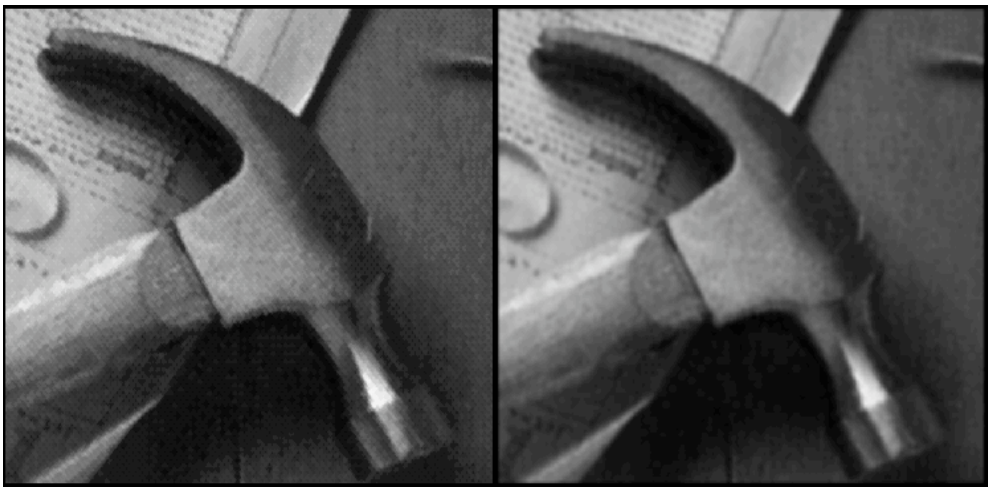

Figure 8: Reconstructed image for 360 DPI target. Single convolution (on the left) and double convolution (on the right).

References

1. M. Analoui and J. P. Allebach, "New results on reconstruction of continuous-tone from halftone," in *IEEE Int. Conf. Acoustics, Speech, Signal Processing*, vol. 3, San Francisco, CA, 1992, pp. 313–316.
2. S. Hein and A. Zakhor, "Halftone to continuous-tone conversion of error-diffusion coded images," *IEEE Trans. Image Processing*, vol. 4, pp. 208–216, Feb. 1995.
3. Z. Fan, "Retrieval of images from digital halftones," *ISCAS*, pp. 313–316, May 1992.
4. P. W. Wong, "Inverse halftoning and kernel estimation for error diffusion," *IEEE Trans. Image Processing*, vol. 4, pp. 486–498, Apr. 1995.
5. Z. Xiong, K. Ramchandran, and M. Orchard, "Inverse halftoning using wavelets," in *Proc. Int. Conf. Image Processing*, vol. I, Lausanne, Switzerland, 1996, pp. 569–572.
6. T. Kite, N. D. Venkata, B. Evans, and A. C. Bovik, "A high quality, fast inverse halftoning algorithm for error diffused halftones," in *Proc. ICIP*, Chicago, IL, 1998.
7. Murat Messe, P. P. Vaidyanathan, "Optimized Halftoning Using Dot Diffusion and Methods for Inverse Halftoning", *IEEE Trans. Image Processing*, vol. 9, No 4 , pp. 691–709, Apr. 2000
8. Jiebo Luo, Ricardo de Queiroz, and Zhigang Fan, "A robust technique for image descreening based on the wavelet transform", *IEEE Trans. Signal Processing*, vol. 46, No 4 , pp. 1179–1180, Apr. 1998
9. Robert Ulichney. Digital Halftoning, The MIT Press, Cambridge Massachusetts. ISBN 0-262-21009-6.
10. D. Kermisch and P. G. Roetling, "Fourier spectrum of halftone images," Journal of the Optical Society of America, vol. 65 pp. 716-722, June 1975.
11. Xiangdong Liu, "Analysis and Reduction of Moiré Patterns in Scanned Halftone Pictures", Diddertation submitted to the faculty of Virginia Polytechnic Institute and State University., May 1996.
12. Ravishankar Rao, Gerald Robert Thompson, Charles Philipe Tresser, Chai Wah Wu, "Printer Dependent Descreening Method", US patent 6,172,769, Jan 2001.
13. Daniel Seidner, Dan Eylon, "Apparatus & and Method for Descreening", US patent 5,333,064, Jul. 26
14. Zhigang Fan, "Unscreening of stored digital halftoned images by logic filtering", US patent 5,027,78, Jun 1991.
15. Jiebo Luo, Ricardo de Queiroz, Zhigang Fan, "Universal Descreening Technique via Wavelet Analysis", 1997
16. Sorn Forchhammer and Kim S. Jensen, "Data Compression of Scanned Halftone Images", IEEE Trans. On Comm. Vol 42, 1994.